Electronic Supplementary Material (ESI) for Lab on a Chip.

Graphene-based microfluidic perforated microelectrode arrays for retinal electrophysiological studies

Alberto Esteban-Linares,[a,‡] Xiaosi Zhang,[b,‡] Hannah H. Lee,[c] Michael L. Risner,[c] Sharon M. Weiss,[b,d] Ya-Qiong Xu,[b,d] Edward Levine,[c,e,*] and Deyu Li[a,*]

[a]*Department of Mechanical Engineering, Vanderbilt University, Nashville, TN, 37235, United States*
[b]*Department of Electrical and Computer Engineering, Vanderbilt University, Nashville, TN 37235, United States*
[c]*Department of Ophthalmology and Visual Sciences, Vanderbilt Eye Institute, Vanderbilt University Medical Center, Nashville, TN, 37232, United States*
[d]*Department of Physics and Astronomy, Vanderbilt University, Nashville, TN, 37235, United States*
[e]*Department of Cell and Developmental Biology, Vanderbilt University, Nashville, TN 37235, United States*
‡These authors contributed equally to this work.
*Corresponding authors: ed.levine@vumc.org; deyu.li@vanderbilt.edu

Table of Contents

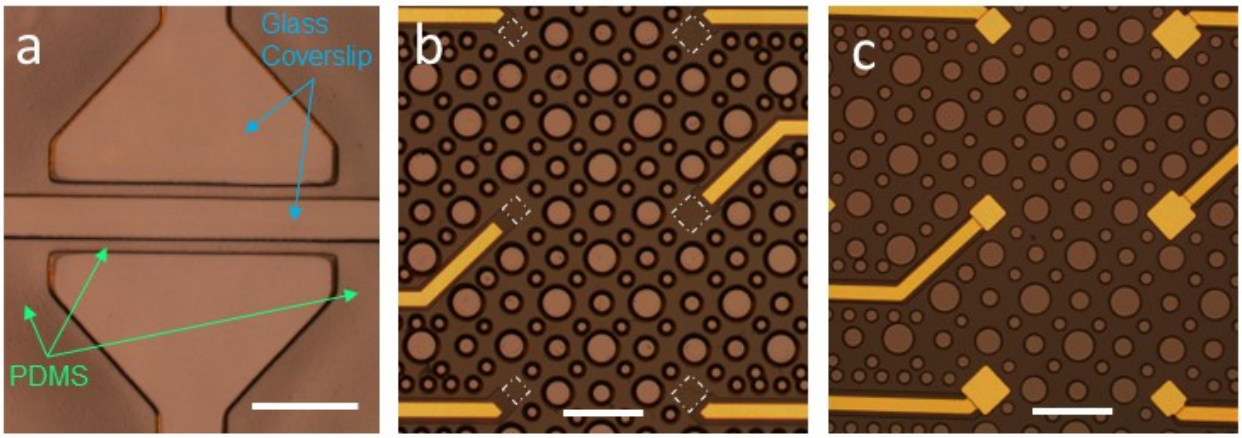

Supplemental Figure 1: Optical images of the μpMEA platform. (**a**) Open Channel PDMS Layer. PDMS structures (green arrows) on a glass coverslip outline the microfluidic channel and chambers. (**b**) The PI layer with through-holes with the graphene electrodes indicated by white dashed boxes. (**c**) An optical image of the microfabricated PI layer with through-holes and Ti/Au electrodes. Scale bars in (**a**), (**b**), and (**c**) are 500, 100, and 100 μm, respectively.

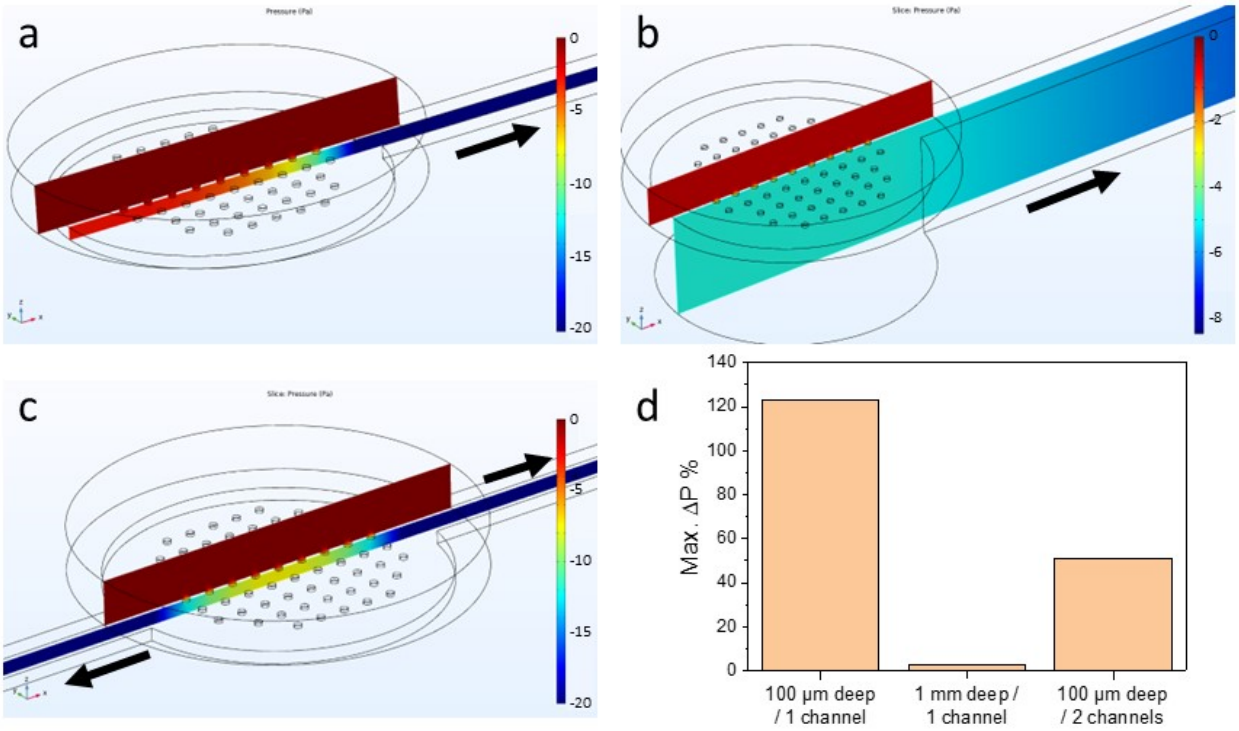

Supplemental Figure 2: COMSOL Multiphysics simulation. Results of three-dimensional computational fluid dynamics model for understanding pressure distribution across the through-holes in three different configurations: one 100 µm deep suction channel (**a**), one 1 mm deep suction channel (**b**), and two 100 µm deep suction channels (**c**). The plot depicts the pressure distribution along a *y*-axis slice at the center of the channel and chamber. (**d**) Statistical analysis results of the pressure distribution across the through-holes in three different configurations, showing a maximum percentage difference in pressure between the holes experiencing the highest and lowest negative pressure of 122%, 3%, and 55%, respectively.

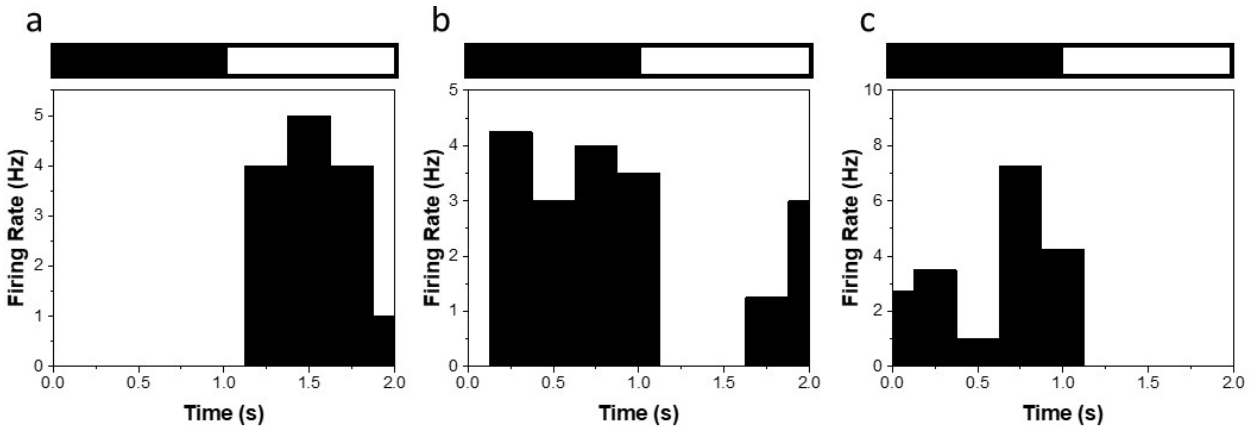

Supplemental Figure 3: Firing activities of three different types of RGCs upon light stimulation: ON Type (**a**), ON-OFF Type (**b**), and OFF Type (**c**) in response to the same light stimulus. Bars above the plots indicate the light OFF (black) and ON (white).

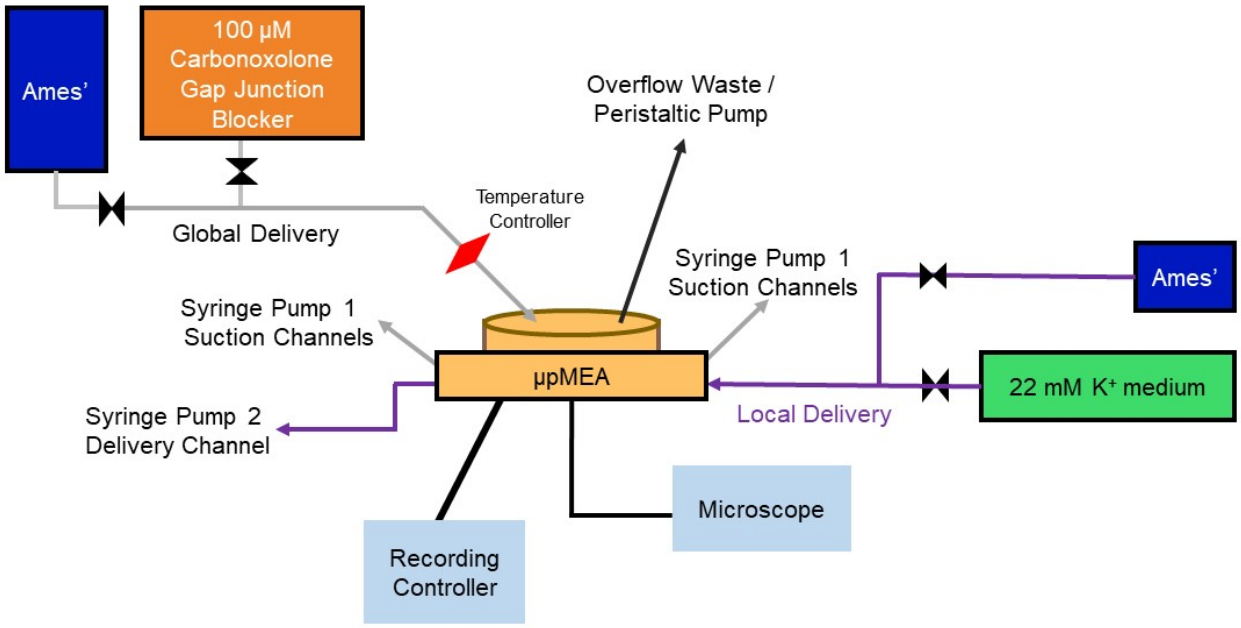

Supplemental Figure 4: Schematic of the experimental design used for the retina pharmacology experiments.

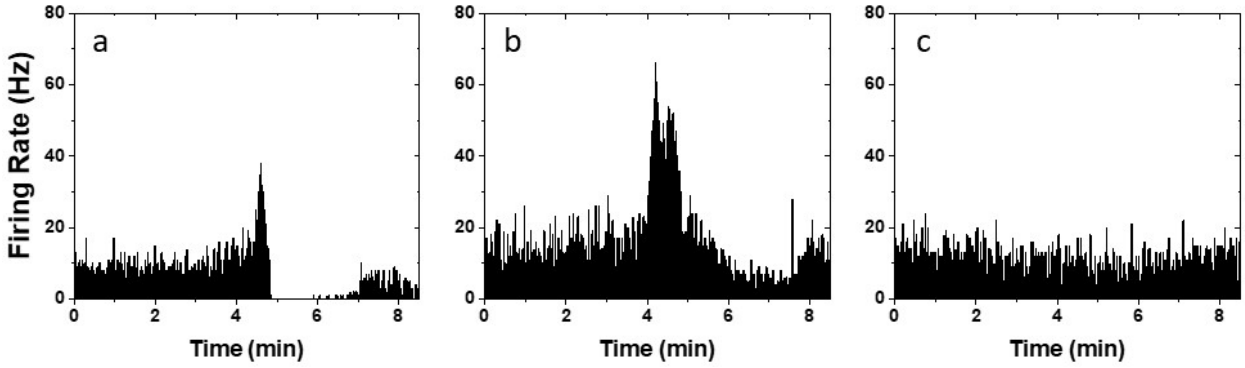

Supplemental Figure 5: Responses of electrodes located away from delivery channel upon locally delivered 22 mM K^+ stimulation. The responses can be categorized as stron (**a**), mild (**b**) and weak (**c**), based on their degree of similarity to standard activity upon high K^+ stimulation (Figure 5c).

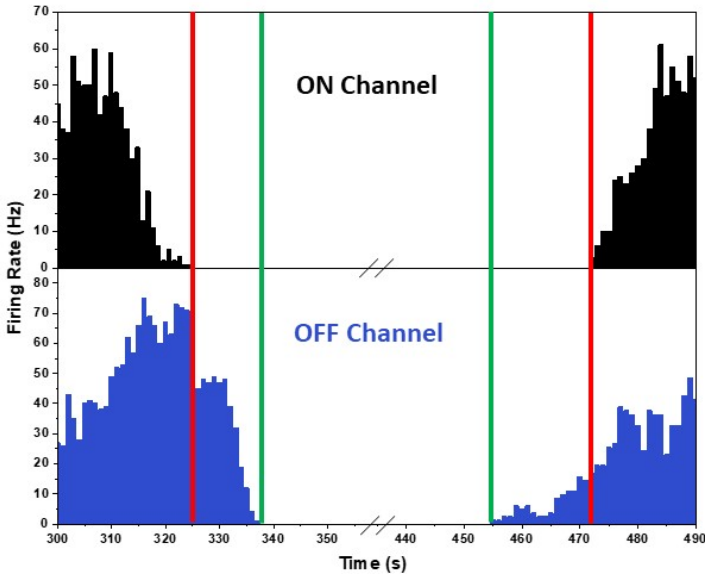

Supplemental Figure 6: Time analysis. Comparison of response to locally delivered K^+ stimulation from electrode located ON (positioned on) and OFF (160 μm away from) the delivery channel. Neuronal depolarization block occurs 12.5 s earlier in the ON channel electrode, whereas the reappearance of firing activity takes place 17 s later. The red and green lines depict the cessation and recovery of action potentials from the electrodes located on and off the delivery channel, respectively.